TRAINED NNU-NET MODEL FOR SEMANTIC SEGMENTATION OF HUMAN ADULT CERVICAL VERTEBRAE FROM CT-SCANS

L. DIOTALEVI [1,2,3], P. LÉGER [1,2,3], M-H. BEAUSÉJOUR [1,2,3], J-M. MAC-THIONG [3,4], AND Y. PETIT [1,2,3]

1. École de technologie supérieure, Montreal, QC, Canada
2. International Laboratory on Spine Imaging and Biomechanics (iLab-Spine)
3. CIUSSS-NÎM research center, Montreal, QC, Canada
4. Université de Montréal, Montreal, QC, Canada

The content of this conference poster was presenting the following paper: L. Diotalevi, P. Léger, M. -H. Beauséjour, J. -M. Mac-Thiong and Y. Petit, "Trained nnU-Net model for semantic segmentation of human adult cervical vertebrae from CT-Scans," *2025 47th Annual International Conference of the IEEE Engineering in Medicine and Biology Society (EMBC)*, Copenhagen, Denmark, 2025, pp. 1-7, doi: 10.1109/EMBC58623.2025.11253480.

INTRODUCTION

The need for automatic segmentation of the spine keeps rising [1]

Patient-based and population-based finite element models of the cervical spine used to perform **numerical simulations require perfectly segmented vertebral geometries** from CT-Scans [2, 3]

Various segmentation models already exist, but always exhibit **low performance on the cervical spine** [4-8]

Cervical vertebrae are morphologically different than thoracic and lumbar vertebrae, which might explain low local performance

nnU-Net is an adaptive versatile semantic segmentation method frequently used in medical images analyses [9]

HYPOTHESIS

Training a semantic segmentation model specifically on the cervical spine segment could lead to better local segmentation performance than using a segmentation model trained on the full spine

Both approaches will be compared, using nnU-Net v.2 trained on publicly available datasets

METHODS

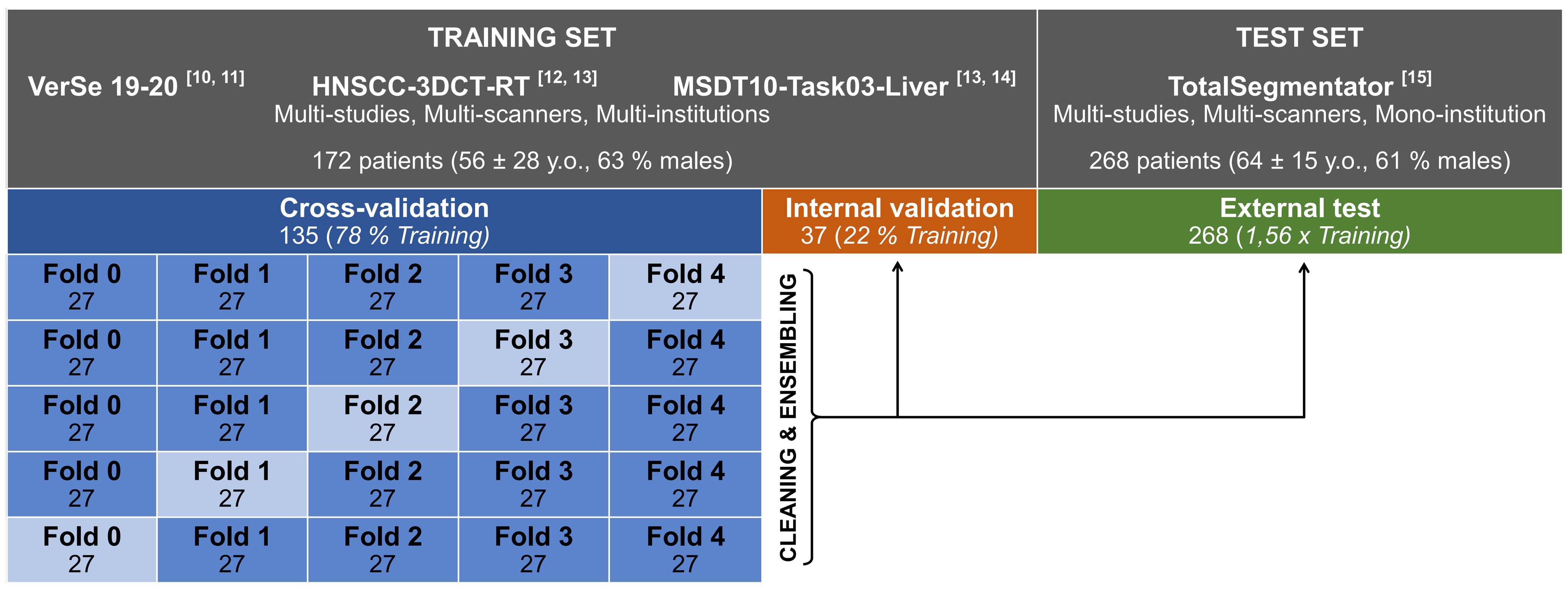

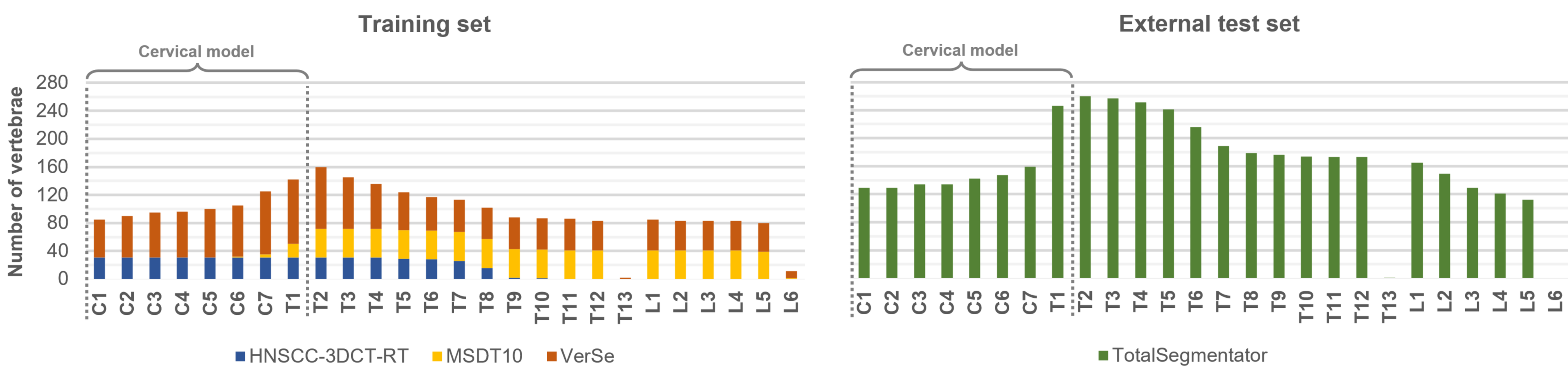

RESULTS: SPECIFIC EXAMPLES AND GLOBAL PERFORMANCE

Female - 22 y.o. - 0.27x0.27x1.25 mm
Low contrast bone / soft tissues

Male - 71 y.o. - 1.27x1.27x2 mm
Massive osteophytic features

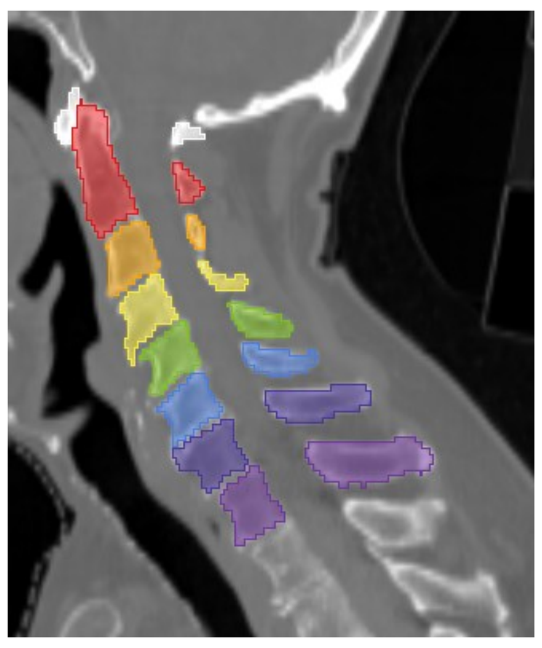

Male - 35 y.o. - 2x0.68x0.68 mm
Full-spine field of view, face erased

Female - 88 y.o. - 1.5x1.5x1.5 mm
Face wrapped

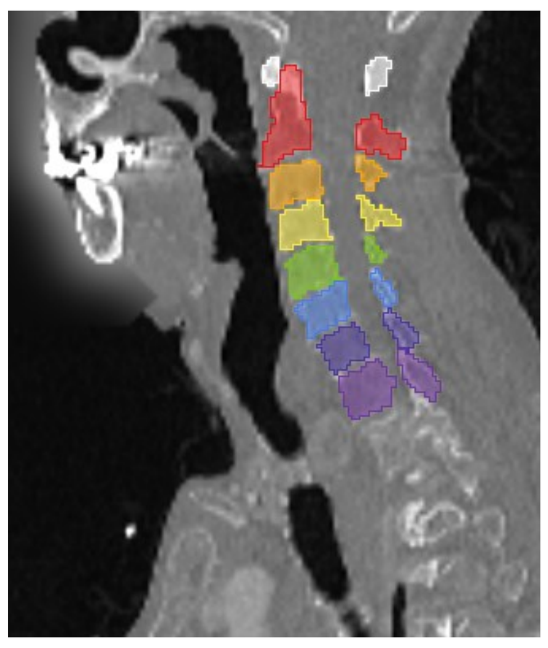

Male - 47 y.o. - 1.5x1.5x1.5 mm
Noised image, cervical spine truncated

Vertebrae	Proposed cervical model performance (trained nnU-Net v.2 3d_fullres)						Deng *et al.* [8] model performance		
	DICE			H_{95} (*mm*)					
	Cross-val. [MIN, MAX]	Int. val. μ ± σ	Ext. test μ ± σ	Cross-val. [MIN, MAX]	Int. val. μ ± σ	Ext. test μ ± σ	Test_public DICE / H_{95}	Test_private DICE / H_{95}	Test_VerSe DICE / H_{95}
C1	[0.937, 0.952]	0.947 ± 0.018	0.959 ± 0.022	[0.90, 1.22]	1.00 ± 0.28	1.28 ± 0.77	0.951 / 1.55	0.957 / 1.34	0.446 / 1.69
C2	[0.953, 0.959]	0.959 ± 0.015	0.962 ± 0.041	[0.89, 1.02]	0.99 ± 0.44	1.25 ± 0.88	0.974 / 1.15	0.975 / 1.22	0.923 / 1.20
C3	[0.929, 0.948]	0.895 ± 0.196	0.943 ± 0.032	[0.94, 1.47]	3.17 ± 7.58	1.74 ± 1.29	0.934 / 8.73	0.945 / 7.55	0.605 / 1.32
C4	[0.922, 0.944]	0.890 ± 0.192	0.938 ± 0.046	[0.95, 1.48]	1.92 ± 2.76	1.50 ± 0.90	0.946 / 1.90	0.608 / 3.65	0.613 / 0.95
C5	[0.929, 0.943]	0.903 ± 0.154	0.941 ± 0.036	[0.99, 1.36]	1.80 ± 2.35	1.72 ± 1.29	0.573 / 2.43	0.726 / 3.13	0.231 / 0.95
C6	[0.872, 0.935]	0.923 ± 0.068	0.943 ± 0.027	[1.12, 3.21]	1.83 ± 2.24	1.42 ± 0.69	0.802 / 4.51	0.824 / 2.38	0.121 / 1.07
C7	[0.822, 0.952]	0.941 ± 0.025	0.957 ± 0.022	[1.08, 8.96]	1.27 ± 0.84	1.27 ± 0.59	0.930 / 2.18	0.899 / 2.16	0.228 / 4.04
T1	[0.872, 0.956]	0.953 ± 0.022	0.961 ± 0.089	[1.52, 3.25]	1.10 ± 0.70	1.32 ± 2.56	0.952 / 1.60	0.927 / 2.36	0.623 / 2.53
[C1, T1]	-	0.928 ± 0.111	0.951 ± 0.051	-	1.60 ± 2.99	1.43 ± 1.44	-	-	-
[C1, L6]	-	-	-	-	-	-	0.869 / 5.40	0.840 / 6.41	0.619 / 6.23

Vertebrae	Cervical model *vs.* Full spine model (two-sided Mann-Whitney U-tests)			
	DICE		H_{95} (*mm*)	
	Int. val. p-value	Ext. Test p-value	Int. val. p-value	Ext. Test p-value
C1	0,759	0,188	0,558	0,063
C2	0,745	0,317	0,655	0,395
C3	0,503	0,395	0,751	0,211
C4	0,707	0,138	0,733	0,180
C5	0,720	0,744	0,669	0,509
C6	0,660	0,712	0,721	0,424
C7	0,608	0,873	0,509	0,843
T1	0,783	0,065	0,441	0,860
[C1, T1]	0,338	0,379	0,184	0,037

CONCLUSION

Results show better performance results than the literature [4-8] for both the cervical and full-spine models

Both presented models show similar performance results

Unlike ours, **models in the literature were trained with unbalanced labels**[4-8]. This might explain why **our models both perform similarly, but way better than the litterature**

Our models were *not* trained *nor* tested on a pediatric population, and *neither* on fractured, metastatic or instrumented vertebrae

REFERENCES

[1] A. Sekuboyina et al., "VerSe: a vertebrae labelling and segmentation benchmark for multi-detector CT images," Medical image analysis, vol. 73, p. 102166, 2021
[2] Y. H. Kim, B. Khuyagbaatar, and K. Kim, "Recent advances in finite element modeling of the human cervical spine," Journal of Mechanical Science and Technology, vol. 32, pp. 1-10, 2018.
[3] Z. Liang, K. Wu, T. Tian, and F. Mo, "Human head–neck model and its application thresholds: a narrative review," International Journal of Surgery, vol. 111, no. 1, pp. 1042-1070, 2025.
[4] A. Sekuboyina et al., "VerSe: a vertebrae labelling and segmentation benchmark for multi-detector CT images," Medical image analysis, vol. 73, p. 102166, 2021.
[5] C. Payer, D. Stern, H. Bischof, and M. Urschler, "Coarse to Fine Vertebrae Localization and Segmentation with SpatialConfiguration-Net and U-Net," in Proceedings of the 15th International Joint Conference on Computer Vision, Imaging and Computer Graphics Theory and Applications (VISIGRAPP), Valletta, Malta, 2020, vol. 5, pp. 124-133.
[6] D. Meng, E. Mohammed, E. Boyer, and S. Pujades, "Vertebrae localization, segmentation and identification using a graph optimization and an anatomic consistency cycle," in International Workshop on Machine Learning in Medical Imaging, Singapore, Singapore, 2022: Springer, pp. 307-317.
[7] J. Wasserthal et al., "TotalSegmentator: robust segmentation of 104 anatomic structures in CT images," Radiology: Artificial Intelligence, vol. 5, no. 5, 2023.
[8] Y. Deng et al., "CTSpine1K: a large-scale dataset for spinal vertebrae segmentation in computed tomography," arXiv arXiv:2105.14711v4 [eess.IV], 2021.
[9] F. Isensee, P. F. Jaeger, S. A. Kohl, J. Petersen, and K. H. Maier-Hein, "nnU-Net: a self-configuring method for deep learning-based biomedical image segmentation," Nature methods, vol. 18, no. 2, pp. 203-211, 2021.
[10] J. S. Kirschke, A. Sekuboyina, and M. Löffler. VerSe 2019, The Open Science Framework, 2019, doi: https://doi.org/10.17605/OSF.IO/NQJYW
[11] J. S. Kirschke, M. Löffler, A. Sekuboyina, and H. Liebl. VerSe 2020, The Open Science Framework, 2020, doi: https://doi.org/10.17605/OSF.IO/T98FZ
[12] T. Bejarano, M. De Ornelas-Couto, and I.-B. Mihaylov. Head-and-neck squamous cell carcinoma patients with CT taken during pre-treatment, mid-treatment, and post-treatment (HNSCC-3DCT-RT), The Cancer Imaging Archive, 2018, doi: https://doi.org/10.7937/K9/TCIA.2018.13upr2xf
[13] Y. Deng et al. AFRICAI_MICCAI2024_CTSpine1K, International Conference on Medical Images Computing and Computer Assisted Intervention (MICCAI), 2024. [Online]. Available: https://xnat.health-ri.nl/data/archive/projects/africai_miccai2024_ctspine1k
[14] M. J. Cardoso. Medical Segmentation Decathlon: Generalisable 3D Semantic Segmentation, Medical Segmentation Decathlon, 2018. [Online]. Available: http://medicaldecathlon.com/
[15] J. Wasserthal. Dataset with segmentations of 117 important anatomical structures in 1228 CT images, Zenodo, 2023. [Online]. Available: https://zenodo.org/records/10047292

Research supported by the Natural Sciences and Engineering Research Council of Canada (570314-2022), Fonds de recherche du Québec - Nature et technologie (B2X-333256), and the Medtronic Chair in Spinal Trauma at Université de Montréal